Section A -Research paper

Magnetic Resonance Imaging features of Sellar and Suprasellar Masses

Ahmed Sabry Ragheb [1], Rania Mostafa Almola [1], Samia Ali Taher Elmajdub [2], Rania Mostafa Hassan [1]

[1]Radiodiagnosis Departments, Faculty of Medicine, Zagazig University, Egypt.

[2] Radiodiagnosis Departments, Faculty of Medicine, Tripoli University, Libya.

Corresponding Author: Samia Ali Taher Elmajdub

Email: Erraysk48@gmail.com

Article History: Received: 26.05.2023 **Revised:** 28.06.2023 **Accepted:** 27.07.2023

Abstract:

The sellar and suprasellar region is an anatomically complex area where a spectrum of the possible pathologies is extremely wide, and includes both neoplastic and non-neoplastic masses. The lesions arising not from the pituitary gland itself, but also from vestigial embryological residues or surrounding tissues, that may require different therapeutic approaches. This article reviews the anatomy, embryology, and pathologic processes that occur in this region as well as the MRI imaging findings for these lesions.

Keywords: Sella, Suprsellar, MRI.

DOI: 10.53555/ecb/2023.12.1053

Introduction:

The sellar and suprasellar region is an anatomically complex area where a number of neoplastic, infectious, inflammatory, developmental and vascular pathologies can occur. Despite the broad spectrum of possible neoplastic and no neoplastic lesions, in almost 80% of these lesions are macroadenomas, aneurysms, craniopharyngiomas, meningiomas, or astrocytomas, with other lesions being relatively rare (**1**). Structural MRI represents the gold standard for their diagnosis and characterization, which is able to provide accurate and reliable information about the nature of the lesion, as well as its relationship with the adjacent structures, allowing to formulate proper hypotheses about its nature. Computed tomography (CT) imaging is complementary to MR imaging for the depiction of bony changes, including remodeling or frank bone destruction **(2).**

ANATOMY AND EMBRYOLOGY

The sella turcica is a saddle-shaped depression on the basisphenoid. The borders of this anatomical structure are defined anteriorly by the middle clinoid processes (two small eminences one on either side), while the posterior border is formed by the dorsum sellae which ends at its superior angles with the posterior clinoid processes. The sellar floor is part of the sphenoid sinus

roof, which is covered by dura and separates it from the pituitary gland (**2**).

The sella turcica harbor the pituitary gland, a bean-shaped gland with two distinct lobes: the anterior lobe, also called the adenohypophysis, and the posterior one named neurohypophysis. The anterior lobe, by far the largest part of the gland, is in turn divided into a "pars tuberalis" (rich in capillaries), a "pars intermedia" and a "pars distalis" (being in terms of volume the most prevalent segment of this portion of the gland) **(3).**

The pituitary gland derived embryologically from different tissues, reflected in the pituitary's mechanisms of function. An outpouching of the ectoderm that develops into the anterior lobe of the pituitary gland. In concert, the developing diencephalon, originating from the neuroectoderm, generates an outpouching from the floor of the developing third ventricle that ultimately becomes the posterior lobe of the pituitary gland **(4).** During the development of the adenohypophysis, the ectodermal outpouching is known as Rathke's pouch. The junction between Rathke's pouch and the neurohypophysis defines Rathke's cleft. Certain pathology can arise from aberrant development of this structure, including Rathke's cleft cysts and craniopharyngiomas**(5).**

The parasellar region is composed of the cavernous sinus and Meckel cave, which is located posterior and inferior, while the suprasellar cistern is situated above the sella, which includes the circle of Willis, the anterior inferior third ventricle and hypothalamic region, the optic pathway, the columns of the fornix, and mammillary bodies.

IMAGING:

The optimum imaging of the sella and suprasellar region is with magnetic resonance (MR) imaging. Computed tomography (CT) imaging is complementary to MR imaging for the depiction of bony changes, including remodeling or frank bone destruction. If MR imaging is contraindicated, thin-section imaging is performed by multidetector CT followed by reconstruction. Contrast should be used on all dedicated sella studies (**2**).

On T1- weighted images, the anterior and posterior pituitary are well delineated by the so-called bright spot of the posterior pituitary, the posterior pituitary being hyperintense relative to gray matter despite the absence of contrast **(8).** Although the cause of the increased signal intensity on T1-weighted images is controversial, this may be caused by secretory granules associated with ADH **(2)**.

On T2-weighted images, the anterior and posterior pituitary are isointense to hypointense on T2-weighted images. In the majority of normal subjects, the central portion of the stalk is hyperintense compared to cerebral white matter due to neurosecretory material and surrounded by a peripheral rim of isointensity, thought to represent pars tuberalis. The T2 sequence is helpful in identifying surrounding neurovascular structures, most notably the optic chiasma (6).

The cavernous sinuses are located immediately lateral to the pituitary gland and contain vascular and neuronal elements. Most prominent in the cavernous sinus is the internal carotid artery, which appears hypointense on both T1& T2 weighted images because of the blood flowing through it, cranial nerves III, IV, V1, and V2 sometimes can be visualized as hypointense filling defects by MRI particularly cranial nerve III. It appears iso-signal to white matter surrounded with a hyperintense thin layer of CSF **(7).**

On postcontrast imaging there is homogeneous moderate to avid enhancement of the anterior lobe of the pituitary gland. Enhancement of the posterior pituitary may be difficult to ascertain because it is already hyperintense on precontrast T1-weighted images **(2).**

PATHOLOGICAL DISORDERS:

The volume of central nervous system that is occupied by the sellar and suprasellar regions is quite small but the range of lesion types that arise in those locations is remarkably large. This can be explained in part by the broad divesity of cellular constituents native to sellar and suprasellar areas **(9).**

Ectopic posterior pituitary:

This congenital anomaly results in an aberrant position of the neurohypophysis. It is associated with pituitary dwarfism, delayed skeletal maturation, septo-optic dysplasia, dysgenesis of the corpus callosum, lobar holoprosencephaly, Chiari 1 malformation or a persistent/enlarged craniopharyngeal canal. MRI may show a small anterior pituitary gland with the posterior "bright spot" on T1-weighted imaging (T1WI) located within the upper portion of the infundibulum or the undersurface of the hypothalamus instead of the dorsal portion of the sella **(10) (fig. 1).**

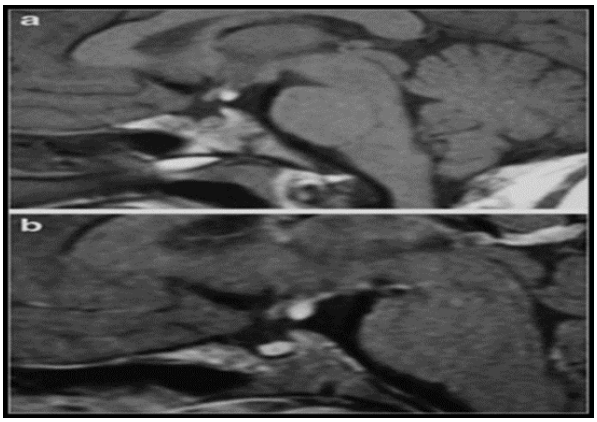

Figure (1): Ectopic posterior pituitary gland. Pre-contrast (a) & post-contrast (b) MR images **(11).**

Hypothalamic hamartomas:

Hypothalamic hamartomas (HHs) represent nonneoplastic congenital gray matter heterotopia arising from the tuber cinereum, it is related to neuronal migration abnormalities. The size of the lesion varies from a few millimeters to huge mixed solid-cystic lesions measuring several centimeters in diameter **(12).** MR imaging showing a sessile or pedunculated mass mainly isointense to the gray matter centered in the tuber cinereum region, without contrast enhancement **(Fig. 2).** The major differential diagnosis is represented by hypothalamic-chiasmatic glioma, which tends to be T1-hypointense and T2-hyperintense, often showing contrast enhancement. No restricted diffusion is seen on DWI. The

absence of growth is seen on follow-up MR examinations **(1).**

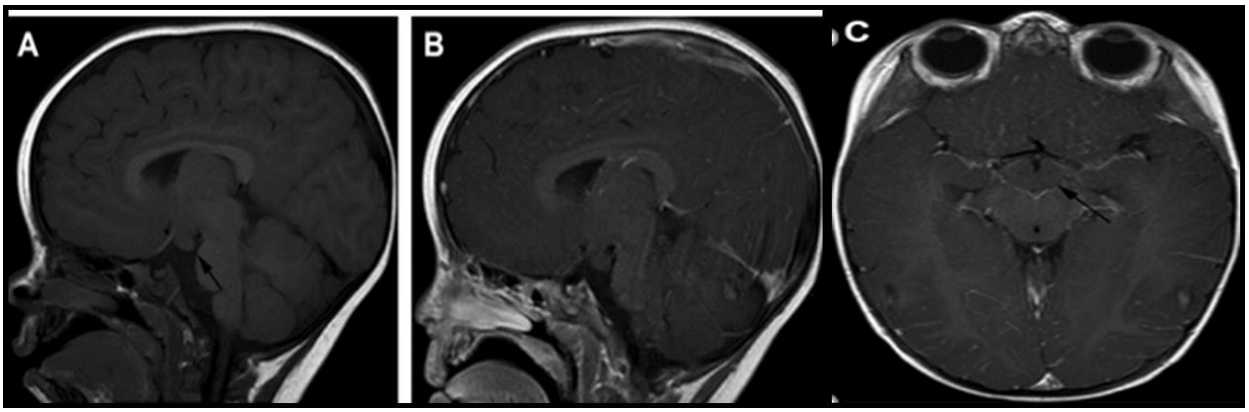

Figure (2): Hypothalamic hamartoma. (A) & (B) Sagittal and axial (C) postcontrast T1WI **(2).**

Rathke cleft cyst:

Rathke cleft cyst (RCC) is a benign lesion arising from remnants of the fetal Rathke pouch. Most RCCs are asymptomatic, and the majority discovered incidentally. Clinical manifestations include headache, pituitary dysfunction, and visual disturbances, due to compression **(13).**

On T1-weighted images, RCCs may present both hypo- or hyperintense; on T2-weighted sequences, about 70% appear hyperintense. An almost pathognomonic feature for RCC is the presence of an intracystic, nonenhancing nodule, showing low intensity on T2- and high intensity on T1-weighted imaging compared to cyst fluid **(Fig. 3).** After contrast administration, an enhancing rim of compressed pituitary surrounding the cyst may give rise to the "claw sign." **(1).** The mean ADC value of the Rathke's cleft cyst relatively high compared to other sellar cystic lesions **(14).**

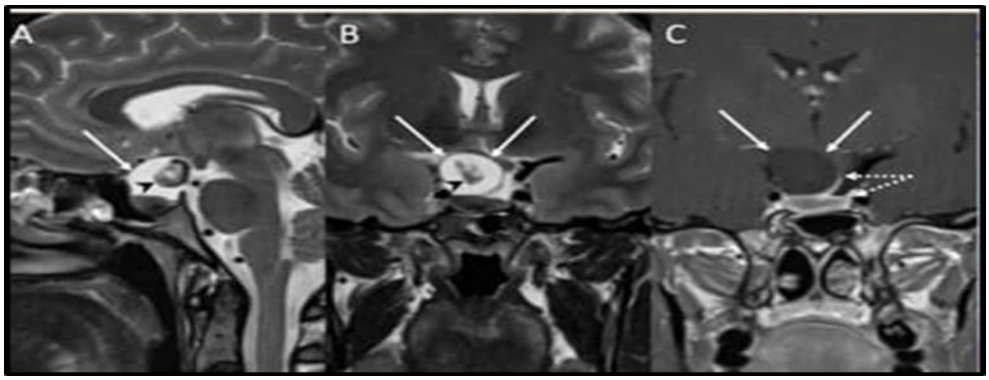

Figure (3) Rathke cleft cyst. Sagittal (A), coronal T2 (B) & contrast-enhanced T1-weighted (C)**(11).**

Arachnoid cyst:

Arachnoid cysts (ACs) represent the most common off midline extra-axial cysts and are usually located within the subarachnoid spaces, including the suprasellar cistern, they are CSF filled lesions **(15).** ACs also follow CSF signal on all MRI sequences **(Fig. 4**). They do not present diffusion restriction nor contrast enhancement. Suprasellar ACs may compress chiasm, pituitary stalk, and/or the third ventricle floor The main differential diagnosis is the epidermoid cyst which however shows higher signal than CSF on FLAIR sequence and diffusion restriction. **(1).**

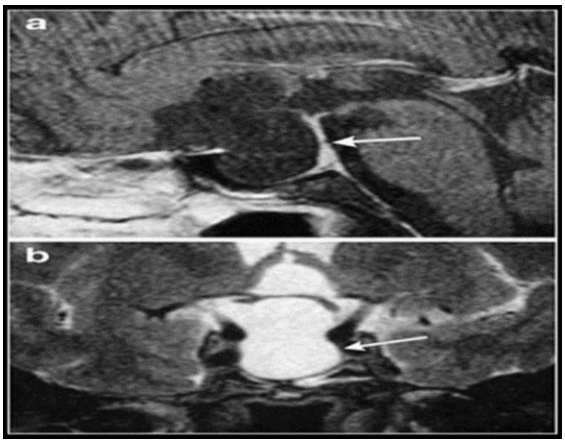

Figure (4): Arachnoid cyst. Sagittal T1WI (a) and coronal T2WI (b) **(11)**.

Pituitary adenoma:

Pituitary adenoma represents the most common masses of the sellar region in adults arising from the adenohypophysis PAs are classified based on their size as macroadenomas (≥ 10 mm) or microadenomas (< 10 mm). Majority of macroadenomas appear isointense to grey matter on T1WI and T2WI **(16) (Fig. 5).**

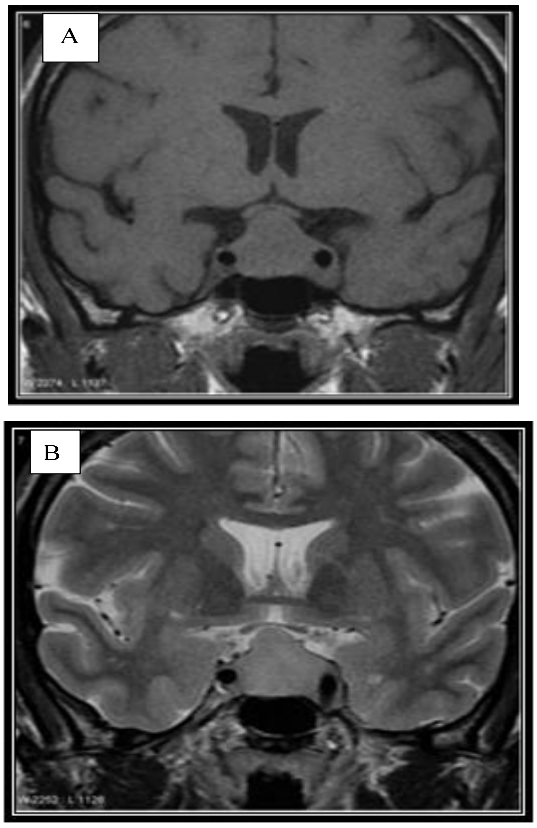

Figure (5): Coronal T1WI (A) & T2WI (B) showing isointense macroadenoma **(17)**.

After contrast media injection, the adenomatous tissue shows intense heterogeneous enhancement and the normal pituitary tissue usually forms a strongly enhancing pseudo capsule around the adenoma. **(19).**

DWI can provide information about the consistency of macroadenomas that cannot be reliably obtained with conventional MR techniques. (The ADC value is inversely proportional to the tumor cellularity) **(20).**

Craniopharyngioma:

Craniopharyngioma (CP) is a benign sellar/suprasellar neoplasm that arises from the anterior part of Rathke pouch, CPs include two distinct entities,

adamantinomatous CP (ACP) and papillary CP (PCP). ACP is significantly more common than PCP (90% vs. 10% of cases, respectively). The clinical manifestations related to the tumor size and mass effect that include headache, visual loss or hydrocephalus, as well as endocrine deficit (e.g., stunted growth, hypogonadism or central diabetes insipidus) **(1).**

On imaging, ACP typically presents as a multilobulated mixed cystic-solid lesion, partially calcified with high-intensity signal on T1-weighted images that results from high protein content. After gadolinium administration, enhancement of the cyst walls and solid components is typical **(fig. 6).** CP typically appear as suprasellar or intraventricular solid, noncalcified mass with smooth margins. Cysts are less common than ACPs. After gadolinium administration, PCP usually shows a relatively homogeneous enhancement **(20).**

Craniopharyngiomas often show no restricted diffusion and high ADC values in consistent with a benign etiology **(21).**

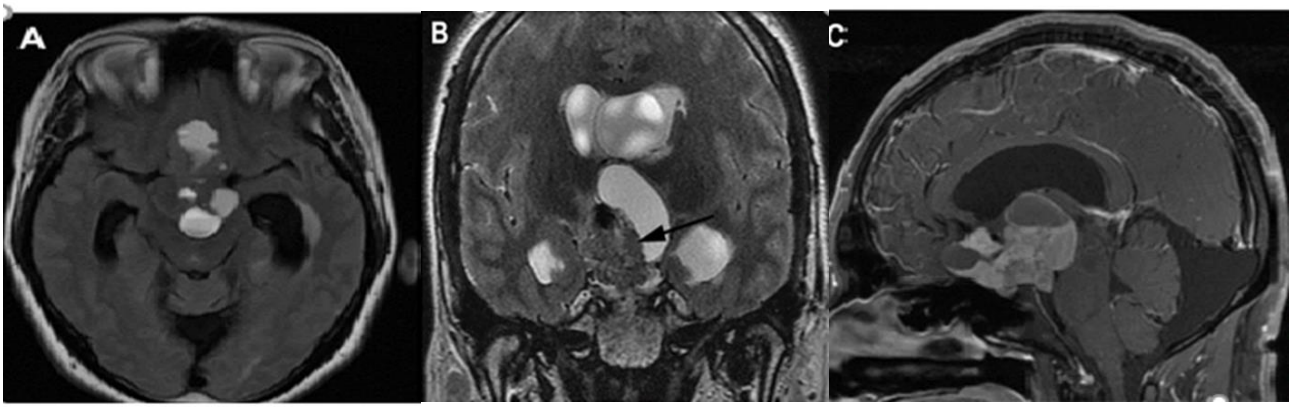

Figure (6): Craniopharyngioma. (*A*) Axial T1WI. (*B*) Coronal T2WI shows solid component (*black arrow*) in addition to the cystic areas. (*C*) The solid components show enhancement in this cystic and solid craniopharyngioma ***(2).***

Meningioma:

Meningioma is the second most common tumor of the sellar region in adults, with an incidence peak between the sixth and the seventh decade of life and female predominance. Meningiomas of this region may arise from the tuberculum sellae, clinoid processes, or cavernous sinus walls. Clinical presentation is related to compression of the surrounding structures, such as visual impairment, endocrine dysfunction, or cranial nerve deficits. On MRI, meningioma appears as a well circumscribed, round or lobulated, extra-axial dura-based mass. It enhances homogenously and brightly ***(22).*** T2-hyperintensity is often associated with a soft consistency, while hypointense tumors tend to be more fibrous and firmer. Reactive thickening of the adjacent dura ("dural tail") ***(23).*** **(fig. 7)**

The benign meningioma showed variable appearance like hypointense, isointense and slightly hyperintense on DWI while malignant/atypical meningiomas returned hyperintense signals on DWI and hypointense in ADC maps **(24).**

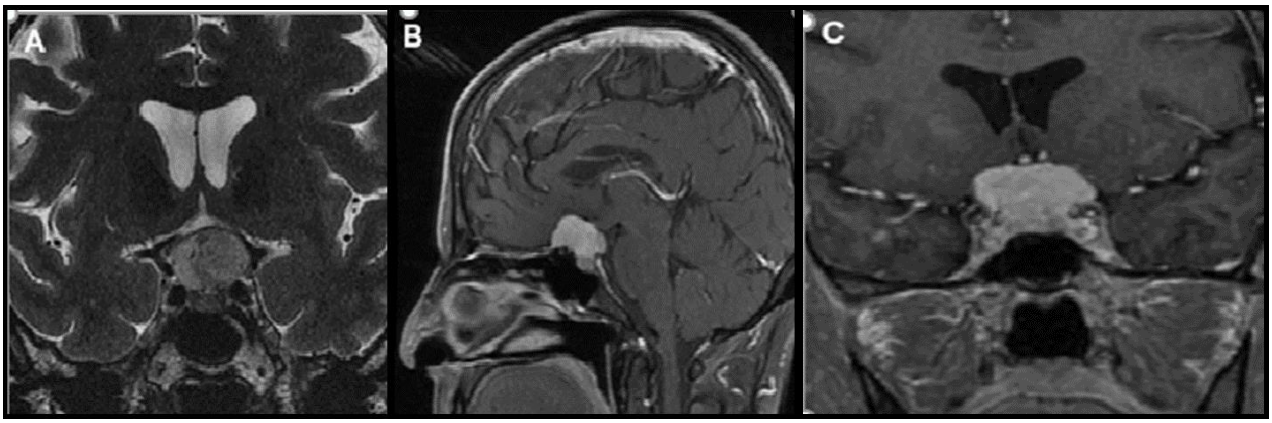

Figure (7): Planum sphenoidale meningioma. (A) T2WI. (B) sagittal, post C T1WI (C) **(2).**

Germ cell tumors (germinoma):

Intracranial germ cell tumors are a heterogeneous group of rare pediatric neoplasms, with peak presentation at 10–14 years of age The first clinical manifestation is often diabetes insipidus, usually occurring before lesions become visible on MRI. Disease progression then result in the development of visual loss, hypothalamic-pituitary dysfunction (with decreased growth and precocious puberty), obstructive hydrocephalus, and in late cases metastatic dissemination via CSF **(25).**

On MRI appear as a well-demarcated infundibular mass with a iso-hyperintense signal on T1W and a slightly low signal intensity on T2-weighted sequences. Moreover, the loss of the normal pituitary bright spot on T1W sequence is a typical feature of sellar germinomas **(26).** Variably sized intratumoral cysts, especially in larger lesions, and calcifications may also be present, with gadolinium enhancement that is strong and usually homogeneous (Fig.8). Given of their hypercellularity and high nuclear to cytoplasmic ratio, germinomas show restricted diffusion on DWI that results in lower ADC values than in other sellar neoplasms. **(1).**

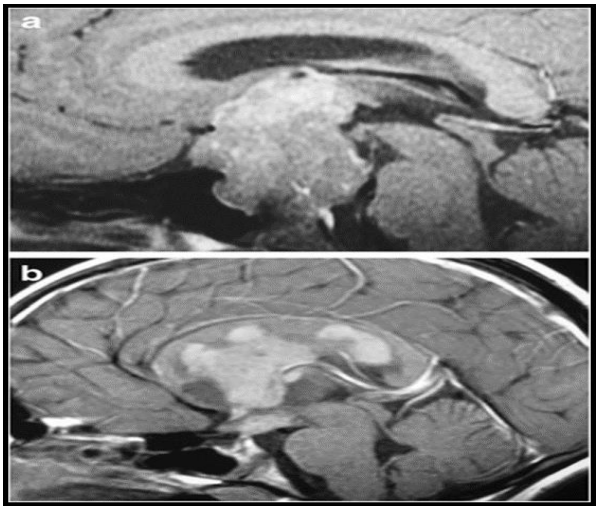

Figure (8): Germ cell tumours in two different children. Post-contrast T1WI (a). Sagittal post-contrast T1WI (b) **(11).**

Optic pathway glioma:

Optic pathway gliomas (OPGs) are low-grade gliomas (WHO grade 1) that arise from the optic pathway or hypothalamus. Onset symptoms are insidious and include visual impairment, pituitary/hypothalamic dysfunction, or hydrocephalus. For this reason, OPGs are often diagnosed late, noticing a visual disturbance progression or exophthalmos for tumors arising from the orbital segment of optic nerve, or nystagmus for OPGs involving the optic chiasm or hypothalamus **(27).**

On MRI, OPGs tend to manifest as T2-hyperintense suprasellar masses, with moderately heterogeneous enhancement **(Fig. 9).** Optic pathway gliomas have high ADC values which related to low cellularity**(28).**

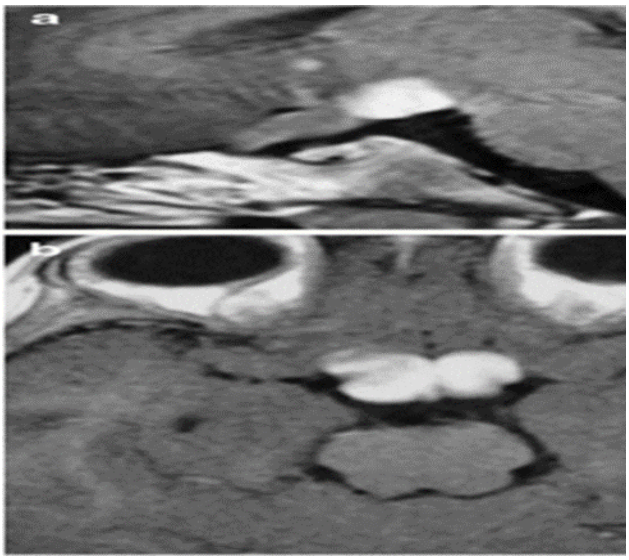

Figure (9): Glioma in a 2-year-old girl with neurofibromatosis type 1. Sagittal (a) and axial (b) post contrast T1WI **(11)**

References:

1. **Ugga L, Franca RA, Scaravilli A, et al., (2023).** Neoplasms and tumor-like lesions of the sellar region: imaging findings with correlation to pathology and 2021 WHO classification. Neuroradiology. 2023 Apr;65(4):675-699.
2. **Go JL, Rajamohan AG (2017).** Imaging of the Sella and Parasellar Region. Radiol Clin North Am. 2017 Jan;55(1):83-101.
3. **Amar AP, Weiss MH (2003).** Pituitary anatomy and physiology. Neurosurg Clin N Am. 2003; 14:11–23. doi: 10.1016/S1042-3680(02)00017-7
4. **Tziaferi V and Dattani MT (2018).** Pituitary Gland Embryology, Anatomy and Physiology. In: Ledbetter D., Johnson P., editors. Endocrine Surgery in Children. Heidelberg, Berlin, Springer; 427-437.
5. **Barkhoudarian G and Kelly DF (2017).** The Pituitary Gland: Anatomy, Physiology, and its Function as the Master Gland. In Cushing's Disease. Academic Press; 10(4): 1-42.
6. **Satogami N, Miki Y, Koyama T et al. (2010).** Normal pituitary stalk: high-resolution MR imaging at 3T. American journal of neuroradiology; 31(2): 355-359.
7. **Bladowska J and Sa˛siadek M (2012).** Diagnostic imaging of the pituitary and parasellar region. In: Movaghar VR., editor. Pituitary adenomas. InTech Europe; 2(1): 13-17.

8. **Côté M, Salzman KL, Sorour M et al. (2014).** Normal dimensions of the posterior pituitary bright spot on magnetic resonance imaging. Journal of neurosurgery; 120(2): 357-362.
9. **Schroeder JW & Vezina LG (2011).** Pediatric sellar and suprasellar lesions. Pediatric radiology, 41, 287-298.
10. **Di Iorgi N, Iorgi ND, Allegri AEM, et al. (2012).** The use of neuroimaging for assessing disorders of pituitary development. Clin Endocrinol (Oxf) 2012; 76:161–176.
11. **Shields R, Mangla R, Almast J, Meyers S (2015).** Magnetic resonance imaging of sellar and juxtasellar abnormalities in the paediatric population: an imaging review. Insights Imaging. 2015 Apr;6(2):241-60.
12. **Wan Chek WAF, Teh YG, Eddy Suryono DN et al. (2021).** MR imaging of hypothalamic hamartoma in a patient with gelastic seizures. Radiol Case Reports 16:2706–2709. https://doi.org/10.1016/j.radcr.2021.06.061
13. **Sala E, Moore JM, Amorin A et al (2018).** Natural history of Rathke's cleft cysts: a retrospective analysis of a two centres experience. Clin Endocrinol (Oxf) 89:178–186. https:// doi. org/ 10. 1111/ cen. 13744.
14. **Kunii N, Abe T, Kawamo M, Tanioka D, Izumiyama H, Moritani T (2007).** Rathke's cleft cysts: differentiation from other cystic lesions in the pituitary fossa by use of single-shot fast spin-echo diffusion-weighted MR imaging. Acta Neurochir (Wien). 2007 Aug;149(8):759-69; discussion 769.
15. **Mustansir F, Bashir S, Darbar A (2018).** Management of arach- noid cysts: a comprehensive review. Cureus. https://doi.org/10. 7759/cureus.2458
16. **Zada G and Lucas J (2013).** Imaging of the Pituitary and Parasellar Region. Seminars in Neurology; 32(04): 320–331.
17. **Bonneville JF (2016).** Nonfunctioning Pituitary Macroadenoma: General Points. In: Bonneville JF., Bonneville F., Cattin F., &Nagi S., editors. MRI of the Pituitary Gland. Springer; 25-33.
18. **Hess CP and Dillon WP (2012):** Imaging the pituitary and parasellar region. Neurosurgery Clinics; 23(4): 529-542.
19. **Thomas T, Gopalakrishnan CV, Thomas B et al. (2014).** Evaluation of consistency of pituitary macroadenoma using diffusion- weighted imaging in correlation with surgical findings. Neurosurgery Quarterly; 24(2): 131-135.
20. **Lubuulwa J, Lei T (2016).** Pathological and topographical clas- sification of craniopharyngiomas: a literature review. J Neurol Surg Reports 77: e121–e127. https://doi.org/10. 1055/s-0036- 1588060.
21. **Soni N, Gupta N, Kumar Y, Mangla M, Mangla R (2017).** Role of diffusion-weighted imaging in skull base lesions: A pictorial review. Neuroradiol J. 2017 Aug;30(4):370-384.

22. **Nowosielski M, Galldiks N, Iglseder S et al (2017).** Diagnostic challenges in meningioma. Neuro Oncol 19:1588–1598. https://doi.org/10.1093/neuonc/nox101.
23. **Guermazi A, Lafitte F, Miaux Y et al. (2005).** The dural tail sign- beyond meningioma. Clin Radiol 60:171–188. https://doi.org/10.1016/j.crad.2004.01.019.
24. **Sohu DM, Sohail S, Shaikh R (2019).** Diagnostic accuracy of diffusion weighted MRI in differentiating benign and malignant meningiomas. Pak J Med Sci. 2019;35(3):726-730.
25. **Partenope C, Pozzobon G, Weber G et al. (2022).** Endocrine manifestations of paediatric intracranial germ cell tumours: from diagnosis to long-term follow-up. Endocrine. https://doi.org/10.1007/ s12020-022-03121-9.
26. **Kilday J-P, Laughlin S, Urbach S et al (2015).** Diabetes insipidus in pediatric germinomas of the suprasellar region: characteristic features and significance of the pituitary bright spot. J Neuroon- col 121:167–175. https://doi.org/10.1007/s11060-014-1619-7.
27. **Aihara Y, Chiba K, Eguchi S et al (2018).** Pediatric optic pathway/ hypothalamic glioma. Neurol Med Chir (Tokyo) 58:1–9. https://doi.org/10.2176/nmc.ra.2017-0081.
28. **Panyaping T, Taebunpakul P, Tritanon O (2020).** Accuracy of apparent diffusion coefficient values and magnetic resonance imaging in differentiating suprasellar germinomas from chiasmatic/hypothalamic gliomas. Neuroradiol J. 2020 Jun;33(3):201-209.